International Journal of Wireless and Mobile Computing

ISSN online: 1741-1092 - ISSN print: 1741-1084
https://www.inderscience.com/ijwmc

Research on adaptive artificial potential field obstacle avoidance technology for unmanned aerial vehicles in complex environments

Hui Li, Xuliang Duan

DOI: 10.1504/IJWMC.2025.10072641

Article History:

Received:	12 October 2024
Last revised:	29 March 2025
Accepted:	10 May 2025
Published online:	06 August 2025

Research on adaptive artificial potential field obstacle avoidance technology for unmanned aerial vehicles in complex environments

Hui Li* and Xuliang Duan

School of Electromechanical and Information Engineering,
Chengdu Agricultural College,
Chengdu, Sichuan, China
Email: lhdxl2005@163.com
Email: 498614712@qq.com
*Corresponding author

Abstract: Path planning for Unmanned Aerial Vehicles (UAVs) in complex environments with coexisting static and dynamic obstacles remains a critical challenge in Artificial Potential Field (APF) research. Current APF methods are constrained by limitations such as target unreachability, local minima entrapment and inefficient dynamic obstacle avoidance, hindering their practical deployment. To address these challenges, an enhanced APF algorithm is proposed, incorporating four key innovations: an adaptive repulsive potential field function to address target unreachability, a randomised directional perturbation strategy for escaping local minima, a collision risk prediction-based force field for dynamic obstacle avoidance, and fuzzy rules with adaptive safety distances to optimise avoidance velocity. Simulation experiments in hybrid static-dynamic obstacle environments demonstrate that the proposed algorithm achieves a 96.3% success rate in trajectory planning with a 3.4 s runtime, 14.79 m path length and maximum angular velocity of 27.89°/s, outperforming conventional APF, DDPG-APF, IAPF, GWO-APF. The collaborative multi-strategy optimisation effectively enhances UAV adaptability in dynamic environments, reduces collision risks and improves trajectory smoothness, providing an efficient solution for real-time path planning in obstacle-dense scenarios.

Keywords: UAVs; unmanned aerial vehicles; APF; artificial potential field; path planning; obstacle voidance technology.

Reference to this paper should be made as follows: Li, H. and Duan, X. (2025) 'Research on adaptive artificial potential field obstacle avoidance technology for unmanned aerial vehicles in complex environments', *Int. J. Wireless and Mobile Computing*, Vol. 29, No. 5, pp.1–12.

Biographical notes: Hui Li is an Associate Professor and Senior Engineer at Chengdu Agricultural College. Her research focuses on agricultural image processing and agricultural unmanned aerial vehicles (UAVs). She has presided over more than 10 projects related to smart agriculture and agricultural UAV technology. She has published over 40 research papers and holds more than 10 authorised patents.

Xuliang Duan is a Senior Engineer at Chengdu Agricultural College. His research focuses on smart agriculture and agricultural unmanned aerial vehicles (UAVs). He has presided over the research and development of radio frequency and microwave technologies for smart agriculture and participated in multiple research projects related to smart agriculture.

1 Introduction

With the rapid advancement of Unmanned Aerial Vehicle (UAV) technology, its applications in military reconnaissance, emergency rescue, mapping inspection, agricultural plant protection and other fields have expanded significantly. However, obstacle avoidance capability during flight remains a critical bottleneck limiting the safety and reliability of UAVs. Therefore, research on UAV obstacle avoidance technologies is essential for enhancing flight system performance.

The Artificial Potential Field (APF) algorithm, a mainstream local obstacle avoidance method, generates collision-free paths for UAVs by constructing virtual potential field functions. Its core principle involves synthesising a total potential field from the attractive force of the target point and the repulsive force of obstacles, guiding the UAV to move along the gradient descent direction. The APF algorithm

is characterised by structural simplicity and intuitive mathematical representation, providing a theoretical framework for real-time UAV path planning. Early studies primarily focused on two-dimensional scenarios. The conventional APF proposed by Li et al. (2024) and Cao et al. (2018) addressed local minima but suffered from global suboptimality due to its greedy strategy. Wei et al. (2023) mitigated trajectory oscillations in narrow channels by dynamically adjusting repulsive coefficients via detection windows, yet remained a local optimisation approach. For multi-obstacle environments, Zhang et al. (2023) introduced virtual force-assisted APF to enhance adaptability in complex scenarios but failed to resolve local minima traps during collaborative obstacle avoidance.

Recent efforts have integrated emerging technologies to improve APF performance. Li et al. (2024) combined APF with optimal consensus control to propose the IAPF algorithm to achieve collaborative obstacle avoidance for multi-UAV systems in unknown environments. Zhou et al. (2023) proposed a hybrid algorithm integrating self-attention-enhanced Soft Actor-Critic (SAC) with APF, significantly improving 3D dynamic obstacle avoidance success rates through real-time trajectory prediction and sparse reward optimisation. Bai et al. (2022) proposed a cooperative trajectory planning method for multiple UAVs based on a Multi-Objective Evolutionary Algorithm (MOEA). By leveraging MOEA to generate Pareto-optimal solution sets, the method balances conflicting objectives (e.g., path length, energy efficiency, collision avoidance) and enhances swarm adaptability in dynamic environments. However, current methods still exhibit limitations. (1) Insufficient model of 3D complex scenarios. Ren et al.'s (2022) distanced threshold method only handles simple obstacle geometries. (2) Weak adaptability to dynamic obstacles. Yao (2020) fuzzy-potential field hybrid algorithm escapes local minima but underperforms in responding to fast-moving targets. (3) Trade-off between global optimality and real-time efficiency. Chen et al. (2024) proposed a GWO-APF method that addresses local minima and dynamic obstacle avoidance limitations, albeit with high computational complexity. Guo et al.'s (2025) DDPG-APF reduces planning time but compromises trajectory smoothness.

Path planning for Unmanned Aerial Vehicles (UAVs) in environments with coexisting static and dynamic obstacles remains a critical challenge in robotics research, particularly due to persistent limitations of Artificial Potential Field (APF) methods, including target unreachability, local minima entrapment and inefficient dynamic obstacle avoidance. This study addresses these shortcomings through four key innovations: (1) An adaptive repulsive potential field function to resolve target unreachability. (2) A randomised directional perturbation strategy enabling escape from local minima. (3) Steering, deceleration and recovery forces triggered by collision risk prediction for dynamic obstacle mitigation. (4) Fuzzy rules with adaptive safety distances to optimise avoidance velocity while controlling computational complexity. Comprehensive simulations in hybrid obstacle environments demonstrate the proposed algorithm's superiority, achieving a 96.3% trajectory success rate with a 3.4 s runtime, 14.79 m path length and 27.89°/s maximum angular velocity, outperforming traditional APF, IAPF and GWO-APF benchmarks. Ablation studies further validate that directional force integration reduces parameterisation demands by 42%, while adaptive fuzzy rules maintain computational efficiency. These advancements collectively enhance UAV adaptability in dynamic settings, offering a robust solution for real-time obstacle-dense navigation. The remainder of this paper is structured as follows: Section 2 details the methodology, Section 3 presents experimental validation and Section 4 discusses implications and future work.

2 Principles and methods

2.1 Principle of artificial potential field

The Artificial Potential Field (APF) method is a path planning technique that models navigation as a force field, where targets generate attraction and obstacles produce repulsion to guide UAV movement. The total potential field, defined as the superposition of gravitational and repulsive fields, directs the UAV along the gradient descent of the potential function to achieve collision-free trajectories (Guo et al., 2025). APF-based obstacle avoidance adapts dynamically to environmental changes with high real-time efficiency (see Figure 1). The proposed UAV obstacle-avoidance framework operates as follows: obstacles in the forward path are first detected. If no obstacles are present, the UAV proceeds along the predefined trajectory to the target. If obstacles are detected, the UAV computes the potential field forces to generate control commands for obstacle avoidance. Upon successful clearance, it resumes the original path. If initial attempts fail, the UAV iteratively recalculates the potential field forces and retries obstacle avoidance until successful passage is achieved.

Figure 1 Flowchart of artificial potential field method

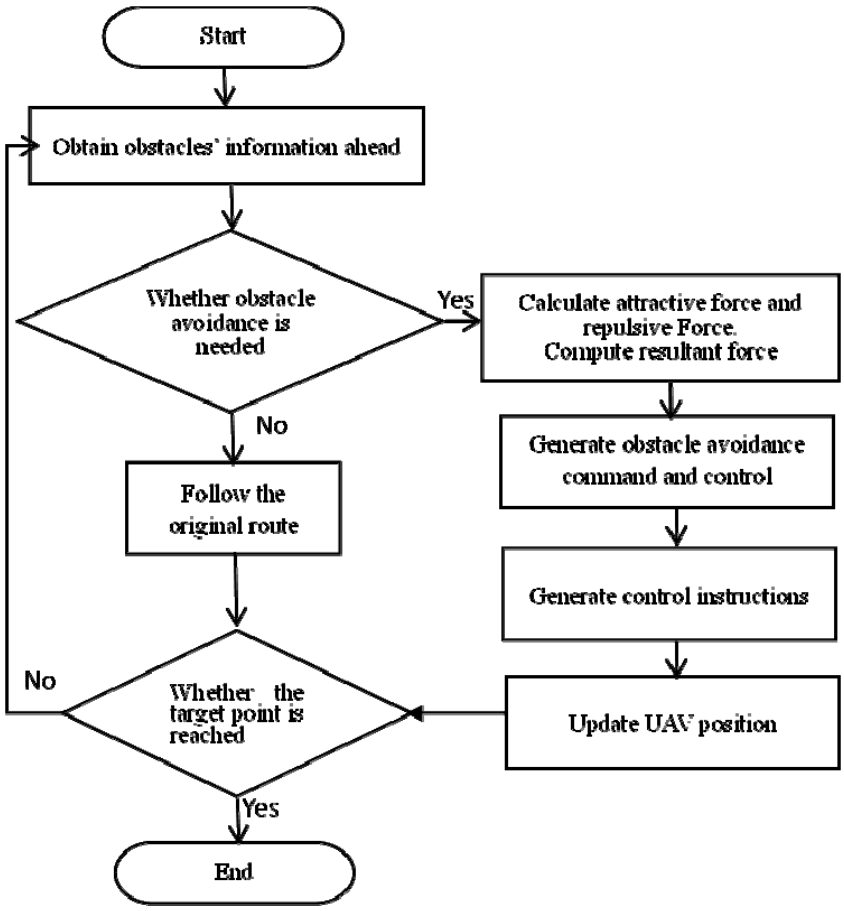

2.1.1 Gravitational function

The gravitational potential field is mainly related to the distance between the drone and the target point, and the larger the distance, the greater the potential energy value experienced by the drone (Xie and Wei, 2020; Jla, 2022; Wang et al., 2021). The gravitational potential field function between the drone and the target point is as follows.

$$U_{att} = \frac{1}{2} k_{att} \left(p - p_g \right)^2 \tag{1}$$

U_{att} is the potential field function of attraction, k_{att} is the proportional gain coefficient of the gravitational field, used to adjust the magnitude of the gravitational force exerted on the UAV. $\left(p - p_g \right)^2$ is a vector, represents the Euclidean distance $\left| p - p_s \right|$ between the position of the UAV p and the position of the target point p_g (Li and Sun, 2023; Wei et al., 2024).

The gravitational force exerted on the UAV at its location is as follow.

$$F_{att}\left(p \right) = grad\left(U_{att}\left(p \right) \right) = -k_{att} \left| p - p_g \right| \tag{2}$$

$F_{att}\left(p \right)$ represents the gravitational field force at position p. $grad\left(U_{att}\left(p \right) \right)$ represents the gradient of the gravitational field U_{att} at position p. It is the direction where the potential energy changes the most at the position in the gravitational field. The direction of the gravitational field force is opposite to the direction of the potential energy gradient.

2.1.2 Repulsive function

The factor determining the repulsive potential field of obstacles is the distance between the UAV and the obstacle. When the UAV does not enter the influence range of the obstacle, its potential energy value is zero. After the UAV enters the influence range of the obstacle, the greater the distance, the smaller the potential energy value received by the UAV (Xie and Wei, 2020; Hou and Kong, 2022; Qin et al., 2024). U_{rep} is a potential field function of repulsive force.

$$U_{rep} = \begin{cases} \frac{1}{2} k_{rep} \left[\frac{1}{\left(p - p_g \right)} - d_{safe} \right]^2, 0 \le \left(p - p_g \right) \le d_{safe} \\ 0, \left(p - p_g \right) \ge d_{safe} \end{cases} \tag{3}$$

k_{rep} is the proportional gain of the repulsive field. Its direction is from the obstacle towards the UAV. d_{safe} is the safe distance threshold. p_0 is the location of the obstacle.

F_{rep} is the repulsive force experienced by the UAV at the location of p. Its function is indicated in function (4).

$$F_{rep}=\begin{cases}-k_{rep}\left(\dfrac{1}{p-p_{\mathrm{g}}}-\dfrac{1}{d_{safe}}\right)^{2}\dfrac{p^{n}{}_{\mathrm{g}}}{(p-p_{0})},(p-p_{0})\le d_{safe}\\ 0,(p-p_{\mathrm{g}})\ge d_{safe}\end{cases} \quad (4)$$

2.1.3 Composite force field function

When the UAV moves towards the target point, it will be subjected to the combined effects of gravitational and repulsive fields. $U(p)$ is the composite potential field. Its function is as follows.

$$U(p)=U_{att}(p)+U_{rep}(p) \quad (5)$$

The resultant function is as follows.

$$F_{total}=F_{att}+\sum_{i}F_{rep}^{i} \quad (6)$$

F_{rep} is the total repulsive force of all obstacles. F_{att} is the attractive force generated by the target point. F_{total} is the force obtained by the principle of force superposition, which is the combined force of repulsive and attractive forces received by the drone. It is the number of obstacles.

Traditional APF method only considers the motion of drones under the influence of the gravitational potential field at the target point and the repulsive potential field of obstacles, resulting in problems such as unreachable targets, local minima, slow obstacle avoidance speed and oscillatory motion trajectories. This study aims to address the aforementioned issues by improving the APF method in a three-dimensional scene, by enhancing the repulsive function to solve the problem of unreachable targets. When the drone is trapped in a local minimum area, the strategy of adding random directional perturbations in the repulsive direction is used to make the drone escape from the local minimum area and solve the problem of local minimum. Introducing steering force to change the speed direction of the drone flying around obstacles, introducing deceleration force to slow down the drone to ensure safety and introducing restoring force to guide the drone back to the pre-determined trajectory to reduce oscillation. Fuzzy rules based on adaptive safe distance improve obstacle avoidance speed and enhance the algorithm's path planning ability in dynamic environments.

2.2 Improving the APF algorithm

2.2.1 Solving the problem of unreachable targets by improving the repulsive function

The fundamental reason for the problem of unreachable targets is that the potential field value at the target point is not the minimum value of the total potential field (Jiang, 2023). As the drone approaches the target point, the gravitational field it experiences decreases while the repulsive field rapidly increases. The resultant force points in a direction away from the target point, causing unexpected adjustments to the flight path and preventing it from reaching the target point. This may even result in path backtracking, reducing the safety of drone flight. Solving the problem of unreachable targets by improving the repulsive function. Divide the repulsive force from obstacles in the artificial potential field method into two parts, F_{rep1} and F_{rep2}, to guide the drone away from the obstacles.

$$\begin{cases}F_{rep1}=nk_{rep}\left(\dfrac{1}{p-p_{0}}-\dfrac{1}{p_{0}}\right)\dfrac{p_{g}^{n}}{(p-p_{0})^{2}}\\ F_{rep2}=\dfrac{n}{2}k_{rep}\left(\dfrac{1}{p-p_{0}}-\dfrac{1}{d_{safe}}\right)^{2}p_{g}^{n-1}\end{cases} \quad (7)$$

n is the repulsive gain coefficient. When n=1, F_{rep1} and F_{rep2}, are respectively represented as follows.

$$\begin{cases}F_{rep1}=k_{rep}\left(\dfrac{1}{p-p_{0}}-\dfrac{1}{p_{0}}\right)\dfrac{p_{g}}{(p-p_{0})^{2}}\\ F_{rep2}=\dfrac{1}{2}k_{rep}\left(\dfrac{1}{p-p_{0}}-\dfrac{1}{d_{safe}}\right)^{2}\end{cases} \quad (8)$$

When the UAV approaches the target point, $p-p_0$ decreases and tends towards zero. The F_{rep1} received by the UAV also tends to zero, and the UAV only moves towards the target direction under the influence of gravity. When $n>1$, as the UAV approaches the target point, $p-p_0$ and p_g^{n-1} approach zero and the total repulsive force exerted on the UAV approaches zero. The drone could gradually reach the target point.

Figure 2 The problem of unreachable targets in a three-dimensional environment and the improved resultant force model (see online version for colours)

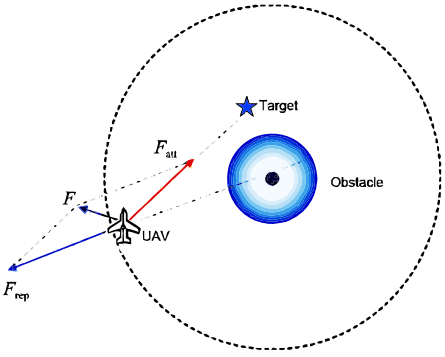

(a) Unreachable targets in three-dimensional space

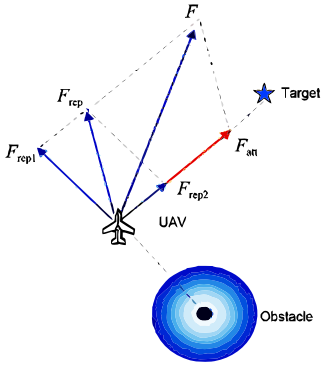

(b) Improved resultant force model

The model of the resultant force in three-dimensional space is illustrated in Figure 2. F_{rep1} and F_{rep2} are the repulsive forces generated by two obstacles. F_{rep} is the total repulsive force of all obstacles. F_{attr} is the gravitational force generated by the target point, and the resultant force F is obtained by the principle of superposition of forces, which is the combined force of repulsion and attraction experienced by the drone.

2.2.2 Local minimum problem

When the drone reaches a collinear position where the gravitational and repulsive forces are equal in magnitude but opposite in direction, the resultant force on the drone is zero or the global minimum, and the drone is trapped in a local minimum area (Xu et al., 2020). Causing the drone to be unable to search for obstacle avoidance paths forward, resulting in the inability to continue moving towards the target point and experiencing stagnation or reciprocating motion. To address this issue, this study introduces directional perturbation strategy when the drone falls into local minimum (Wang, 2023). If the direction perturbation strategy is introduced in all potential fields, it will result in low search efficiency and increase the length of obstacle avoidance. Therefore, when introducing the direction perturbation strategy, only the perturbation condition is added when falling into local extremum. When a drone encounters a local minimum problem, there are two situations: the first is that the minimum point will always appear at a fixed point or hover between two points, causing the combined force of attraction and repulsion to be zero. The second type is that there are obstacles between the current point and the target point, which prevent the drone from reaching the target point. In order to determine whether the drone has fallen into a local minimum, the current point and resultant force position information are recorded separately. If there are more than 5 points that meet the above two conditions, they meet the criteria for falling into a local minimum, and a trajectory adjustment strategy is adopted. Adjust the direction of the trajectory to be consistent with the direction of the repulsive force, and add random directional perturbations in the direction of the repulsive force. Through directional perturbation strategy, jump out of the current local minimum range and continue flying towards the target point. The perturbation function is as follows.

$$F_y = -y / x + rand(\ ) \tag{9}$$

$$F_z = -z / x + rand(\ ) \tag{10}$$

F_y and F_z denote the incremental disturbance forces along the *y*- and *z*-axes, respectively, while *x*, *y* and *z* represent the drone's positional coordinates in the corresponding spatial dimensions. The function $rand(\ )$ generates a random value within a defined range to simulate stochastic perturbations.

2.2.3 Obstacle avoidance problem in dynamic environment

During the flight of the drone, if it exceeds the safe distance of the designated obstacle, it indicates that the drone is already flying in the alert airspace. If it continues to fly at the current speed, there is a possibility of collision, and it must be determined whether to take evasive measures. Fuzzy rules based on adaptive safe distance can improve obstacle avoidance speed and enhance the algorithm's path planning ability in dynamic environments. Assuming that the flight trajectory of the drone intersects with an obstacle. p_u, p_0 and p_g are the real-time position vectors of the drone, obstacle and target point. The safe distance for obstacles is d_{safe}. The speed of the drone is V_U, and the speed of the obstacle is V_0.

$$d = p_u - p_0 \tag{11}$$

The parameter d denotes the relative position vector between the UAV and the obstacle.

$$\alpha = v_u - m \tag{12}$$

α reflects the direction and magnitude of velocity adjustments in obstacle avoidance strategies.

$$\theta = v_0 - d \tag{13}$$

The vector m is represented as follows:

$$m = d - \frac{\|d\| \sin\theta}{\sin\gamma} \cdot \frac{v_0}{\|v_0\|} \tag{14}$$

The angle θ evaluates collision risks induced by the obstacle's motion direction, while γ, the predicted collision angle between the obstacle's boundary vector BA and v_0, quantifies the likelihood of the UAV entering the obstacle's hazardous zone. The vector dynamically adjusts the UAV's intended trajectory by integrating relative position and obstacle motion to avoid collisions. The minimum turning radius $r_{\min}$ constrains the curvature of avoidance paths, and γ, an altitude adjustment parameter implicit in the denominator of equation (17), determines whether the UAV can safely bypass the collision zone from above. The trigonometric functions $\sin\theta$ and $\cos\theta$ characterise directional effects of relative motion based on θ.

$\gamma = \langle BA - v_0 \rangle$ is the collision area where the UAV predicts whether a collision will occur. When the following three obstacle avoidance conditions are met, the UAV will take obstacle avoidance actions. Equation (14) represents the solution process for vector m, where m represents the projection of the relative velocity between the UAV and the obstacle in the direction of the obstacle's velocity. In a dynamic environment, the speed of the UAV V_U and the speed of the obstacle *V*, as well as their real-time positional

relationship, need to be considered when avoiding obstacles. The formula calculates *m* to help determine whether the drone is in danger of collision, and improves obstacle avoidance speed and path planning capabilities based on fuzzy rules and adaptive safety distances. When the obstacle avoidance conditions are met, the drone will take corresponding actions to avoid collisions.

$$d \cdot \sin\theta \le d_{safe} \tag{15}$$

$$\frac{d \cdot \sin\theta \cdot \tan\alpha}{\sin\lambda} \le r_{\min} \tag{16}$$

$$\|v_0\| \sin(\theta + \gamma) \le \|v_u\| \cos\theta \sin\theta \tag{17}$$

Condition (15) indicates that the UAV has flown within the alert airspace. Condition (16) indicates that if the UAV continues to fly at the current speed in the direction, there is a possibility of collision. Condition (17) tests whether the UAV can fly over from the collision frontal height. In this study, in addition to the traditional classification of virtual forces into attractive and repulsive forces, the APF method is improved by introducing three novel forces, which are steering force, deceleration force and restoring force. The steering force is generated by the vector field surrounding the collision area. The deceleration force is utilised to slow down the UAV's flight speed, preventing it from approaching and colliding with obstacles at excessive speeds. Concurrently, the restoring force is enhanced to better guide the UAV back along the preset trajectory.

(1) Introduce steering force F_D to change the speed and direction of the UAV flying around obstacles

$$F_D = \begin{cases} 0, \|d\| \sin\theta > \gamma_{safe} \\ k_\delta \left(\dfrac{1}{d_{safe}} - \dfrac{1}{\|d\| \sin\theta - \gamma_{\min}} \right) \|d\| \sin\theta \le \gamma_{safe} \end{cases} \tag{18}$$

$\delta = \langle d, p_0 \rangle$ is the azimuth angle of ρ relative to p_0. p_0 is the value of ρ at the beginning of the obstacle avoidance process and k_δ is the decreasing function of F_D.

$$k_\delta = \frac{k}{1 - \cos\delta}, \delta \in [0, \pi] \tag{19}$$

k is a constant. F_D has a significant impact on UAV in the initial stage, but as evasion actions progress, its impact on UAV becomes smaller and smaller.

(2) Introduce deceleration force F_S to slow down the UAV to ensure safety

When starting to avoid obstacles, the UAV needs to slow down to avoid collision with obstacles and ensure flight safety. The deceleration force F_S can decelerate the drone to ensure safety.

$$F_S = \begin{cases} \delta \|v_u - v_0\|^{pr} \cdot \dfrac{v_u}{\|v_u\|}, \partial \in \left[0, \dfrac{\pi}{4}\right] \\ 0_0, \partial \in \left[\dfrac{\pi}{4}, \pi\right] \end{cases} \tag{20}$$

$\delta = [0 - 1]$, $\|v_u - v_0\|^{pr}$ is the norm of the projection vector of the difference between v_0 and v_u in the *d* direction. F_S is opposite to v_u direction, producing negative acceleration.

(3) Introduce resilience F_R to guide the UAV back onto the predetermined trajectory and reduce oscillation

UAVs are easily affected by the potential field of obstacles during obstacle avoidance, which can cause them to deviate from the expected trajectory. With the help of the restoring force F_R, the UAV can be guided back to the predetermined trajectory. Adding a deceleration strategy to the F_R model can reduce the oscillation of UAV speed reduction.

$$F_R = \begin{cases} k_1 \cdot n, \|n\| \ge D_1 \\ k_2 \dfrac{\|v_u\| \cos\langle v_u, n \rangle^2}{\|n\| - \lambda D_2} \dfrac{n}{\|v_u\|}, D_2 < \|n\| < D_1 \\ k_3 \|n\|^\mu n, \|n\| \le D_2 \end{cases} \tag{21}$$

D_1 and D_2 are constants. $D_1 \ge D_2$, $k_1 > 0.1$, $k_2 < 0$, $k_3 > 0$. $n = p - p^{pr}$, $p = p_g - p_u$. p^{pr} is the projection vector in the v_g direction. When in the D_1 and D_2 intervals, F_R decelerates the UAV to a given trajectory to overcome the oscillation problem, and the UAV is guided back to the preset flight trajectory with a smaller acceleration.

(4) Joint effort F_{total}

$$F_{total} = F_{att} + F_{rep} + F_D + F_S + F_R \tag{22}$$

The real-time movement of the UAV in the environment is propelled by F_{total}, and the movement step size and total number of steps are set to guide the UAV from the starting point to the ending point.

2.2.4 *Improving obstacle avoidance speed based on adaptive safety distance fuzzy rules*

Considering the different sizes and velocities of obstacles, improve the obstacle avoidance strategy by using velocity parameters and obstacle size parameters to jointly determine the safe collision avoidance distance and speed (Liu, 2023).

(1) *Dealing with obstacles*: During the dynamic obstacle avoidance process of UAV, obstacles of different shapes have a significant impact on the repulsive boundary. Therefore, when using the improved APF method for local planning in this article, the first step is to expand the obstacles. Obstacles of different shapes are processed into spherical obstacles, with the centre of the sphere set as the centre point of the obstacle and the radius of the sphere set to the minimum size that can completely cover the obstacle.

(2) *Set adaptive safety distance*: As shown in Figure 3, to cope with movable obstacles of various sizes and speeds, Unmanned Aerial Vehicles (UAVs) adopt a flexible strategy by setting the safety distance as a variable the

UAV sets the above safety distance as d_{safe} and the variable safety distance as D_{adjust}.

$$D_{adjust} = D_{s\min} + \frac{a * \|v_0\| + b * R}{K} \tag{23}$$

$D_{s\min}$ is the minimum safe distance, and if the distance between the UAV and the obstacle is less than this distance, a collision will occur. $\|v_0\|$ is the velocity of the obstacle, R is the radius of the obstacle, a, b, and K are all constants. Parameter a represents the speed factor, which is used to quantify the impact of obstacle speed on the safety distance. The faster the obstacle, the greater the safety distance that the drone needs to maintain to avoid potential collision risks. Parameter b represents the radius factor, which is used to quantify the impact of the radius of obstacles on the safety distance. The larger the radius of the obstacle, the greater the safety distance that the drone needs to maintain. The parameter k represents the adjustment factor, which is used to scale or adjust the overall safety distance, allowing the drone to more flexibly adjust its flight path when facing obstacles of different speeds and radii. This study is based on experimental data and empirical rules. Set to a=4, b=2 and K=0.8, which can be adjusted according to the actual situation.

Figure 3 Adaptive safety distance (see online version for colours)

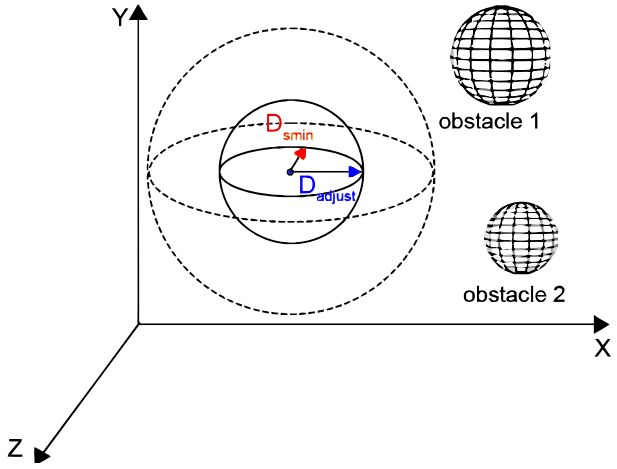

This variable safety distance D_{adjust} can dynamically adjust according to the speed and radius of the obstacles. Specifically, when both the speed and radius of an obstacle increase simultaneously, the safety distance will correspondingly double to ensure that the UAV has sufficient time and space to make obstacle avoidance responses. This is because faster speed and larger volume mean that the obstacle has a stronger dynamic impact range and potential collision energy. In order to ensure that the UAV has enough time and space to make a safe response and avoid collisions, it is necessary to increase the safety distance to cope with this enhanced dynamic threat and ensure the safety and reliability of flight. Conversely, if the obstacle is far away from the UAV, the safety distance will remain within the preset minimum safety distance to reduce unnecessary flight restrictions. Once the obstacle enters within the safety distance, the UAV will immediately sense a repulsive force from the obstacle, triggering the obstacle avoidance mechanism, resulting in a directional deflection or change in speed to effectively avoid the obstacle and ensure the safety and stability of the flight (shown in Figure 3).

(3) *Fuzzy rule setting*: Integrating fuzzy control with APF method enables rapid path planning while mitigating path-obstacle conflicts. This study proposes a speed gain fuzzy controller that dynamically adjusts UAV velocity based on obstacle threat levels and state assessments, facilitating efficient escape from hazardous zones. The controller employs two linguistic input variables: The angle between the UAV-obstacle velocity vectors (domain: [0°, 180°]). The variable safety distance (domain: [5, 15]). The output variable is the UAV speed gain (domain: [0, 0.25]).

The fuzzy system configuration consists of four key components. First, the input variables include the variable safety distance, characterised by fuzzy subsets {LM (Low), M (Medium), H (High)} to represent proximity thresholds, and the velocity vector angle, described by fuzzy subsets {ZEN (Near Zero), NL (Negative Large), N (Negative Small), NH (Positive Small)} to capture relative motion directionality. Second, the output variable, speed gain, is governed by fuzzy subsets {LLA (Extremely Low), LA (Low), MMA (Moderately Low), MA (Moderately High), HHA (High), HA (Extremely High)} to regulate acceleration adjustments. Third, Gaussian membership functions were selected to ensure smooth mapping between variables and fuzzy subsets, enhancing the continuity of the reasoning process (as illustrated in Figure 4). Finally, a 12-rule system, implemented in MATLAB's Fuzzy Logic Toolbox, synthesises expert knowledge and empirical testing to achieve a balance between obstacle avoidance efficacy and flight stability (detailed in Table 1).

This approach ensures robust and adaptive path planning in dynamic environments, leveraging fuzzy logic to enhance the performance of traditional APF methods.

Table 1 Fuzzy rules tables

No.	*Input 1*	*Input 2*	*Output*
1	L	ZE	LA
2	L	NL	LA
3	L	NH	MMA
4	M	ZE	MA
5	M	NL	MMA
6	M	NH	HHA
7	H	ZE	MA
8	H	NL	HHA
9	H	NH	HA

Figure 4 Membership function (see online version for colours)

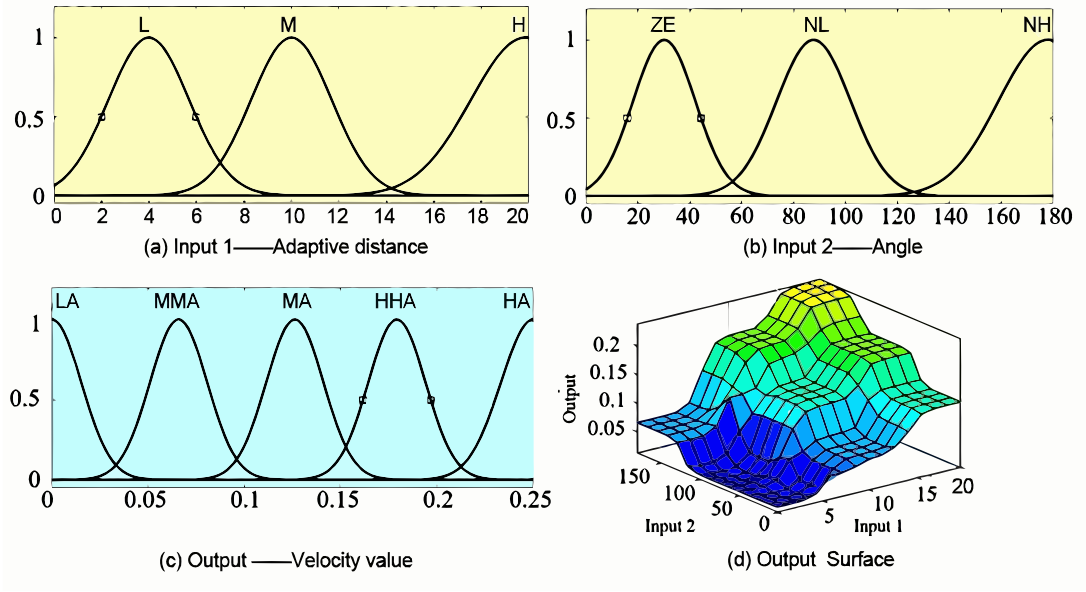

3 Simulation verification and analysis

3.1 Experimental environment

The experimental equipment, environment, and drone flight parameter settings for simulation are shown in the table. Assuming a constant flight rate of the drone, ignoring the interference of natural environmental factors. The simulation experimental equipment and environment are as follows: Inter i7-13700KF, 32GB, dual channel memory, Windows 10 64 bit operating system, Python 3.8.10, Torch 1.14.0, Gym 0.21.0, MATLAB R2022.

The proposed enhanced APF method was validated via MATLAB simulations. Four critical scenarios were systematically evaluated: (1) Target unreachability resolution (2) Local minima mitigation (3) Dynamic obstacle avoidance (4) Multi-algorithm trajectory planning. These experiments demonstrate the method's feasibility and dimensional adaptability across diverse operational constraints.

3.2 Target unreachable test

To verify the problem of unreachable targets, let the starting coordinates of the drone be and the target point coordinates be. Eight obstacles were set up in the spatial environment, and obstacles were also placed next to the target point. Among them, the black pentagram is the starting point, the red pentagram is the target point, the blue sphere is the obstacle and the generated trajectory is the red line. The coordinates of obstacles in the three-dimensional environment are shown in Table 2, and the improved APF parameters are shown in Table 3.

Figure 5 compares the goal-unreachable performance of the conventional Artificial Potential Field (APF) algorithm and the proposed improved method. In Figure 5(a), under the conventional APF framework, the UAV successfully avoids obstacles near the target but fails to reach it due to excessive repulsive forces from adjacent obstacles, despite proximity to the goal. Figure 5(b) demonstrates that the improved algorithm ensures safe target arrival by mitigating repulsive interference, thereby resolving the goal-unreachable problem inherent in the traditional approach.

Table 2 3D coordinates of obstacles for target unreachable experiment

No.	*Coordinate* $[x, y, z]$
1	$[1, 0.5, 0.5]$
2	$[2, 2.5, 2.5]$
3	$[1.3, 2, 1.4]$
4	$[2.5, 1, 1.1]$
5	$[3.3, 2, 2.1]$
6	$[7, 7.2, 7]$
7	$[8, 8, 8]$
8	$[10, 9.5, 9.1]$

Table 3 Parameters of improved artificial potential field method

Simulation parameters	*Value/Unit*
Gravitational gain coefficient κ_{attr}	17
Repulsive gain coefficient η_{rep}	5
Threshold ω	2
Relative velocity gain coefficient κ_v	7
Range of action of obstacles ρ_0	2
Basic step size S	0.02
Maximum iteration number M	1000

Figure 5 Target unreachable experiment before and after APF method (see online version for colours)

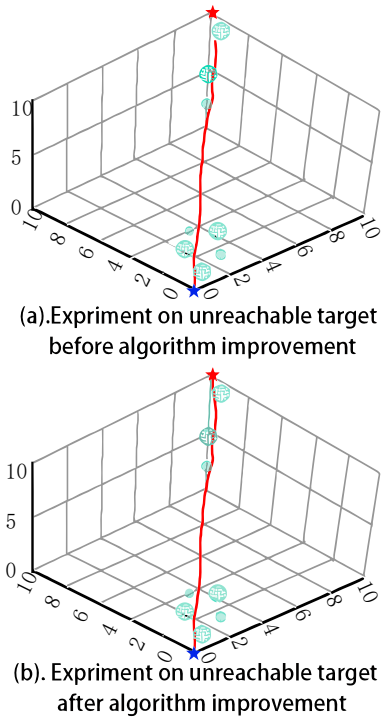

3.3 Local minimum test

To demonstrate the effectiveness of the improved algorithm in solving the local minimum problem, 9 obstacles were set up in the simulation environment, with their coordinate positions shown in Table 4.

Table 4 3D coordinates of obstacles for local minimum test

No.	*Coordinate* $[x, y, z]$
1	[0.5, 0.5, 0.5]
2	[2, 2.5, 2.5]
3	[1.3, 2, 1.4]
4	[2.5, 1, 1.1]
5	[3.3, 2, 2.1]
6	[7, 7.2, 7]
7	[8, 8, 8]
8	[9, 9.5, 9.1]

Figure 6 compares the local minima performance of the conventional Artificial Potential Field (APF) algorithm and the proposed improved algorithm. In Figure 6(a), under the conventional APF framework, the UAV becomes trapped in a local optimum when gravitational and repulsive forces are collinear but opposite, resulting in a zero resultant force and halting obstacle avoidance. Figure 6(b) demonstrates that the enhanced algorithm, incorporating a directional perturbation strategy, effectively resolves this issue, enabling the UAV to safely reach the target and confirming the mitigation of local minima in the proposed method.

Figure 6 Local minima test before and after improvement of APF method (see online version for colours)

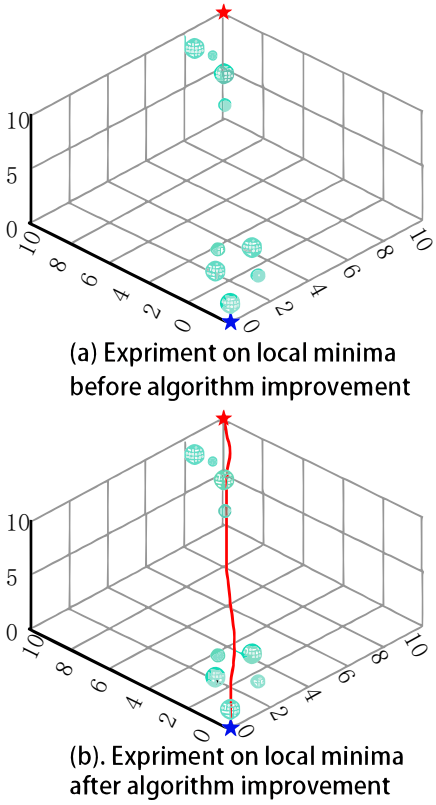

3.4 Obstacle avoidance test in dynamic environment

Simulate and analyse the proposed UAV adaptive APF obstacle avoidance method based on complex environments. The size of the three-dimensional dynamic space is defined as 20 × 20 × 20. The starting coordinates of the drone are [0, 0, 0], the target point coordinates are $[19,19,19]$. The experimental scene includes 4 stationary obstacles and 2 dynamic obstacles. Red spheres represent dynamic obstacles, while blue spheres represent static obstacles. Drones need to avoid obstacles and reach the target location smoothly. The gain coefficients of the gravitational field are $k_{att} = 15$ and $k_{att} = 10$, and the gain coefficients of the repulsive field are $k_{rep} = 10$ and $k_{rep} = 5$, respectively. The parameters of obstacles in the three-dimensional environment are shown in Tables 5 and 6.

Table 5 Parameters of static obstacles in a three-dimensional environment

No.	*Coordinate* $[x, y, z]$	*Radius(r)*
1	[4, 5, 4]	1
2	[8, 9, 9]	0
3	[11, 15, 13]	1.3
4	[14, 11, 6]	2

Table 6 Parameters of dynamic obstacles in a three-dimensional environment

No.	*Initial Position* $[x, y, z]$	*Radius(r)*	*X-axis step size*	*Y-axis step size*	*Z-axis step size*	*Motion period*
1	[6,11,7]	2	0.02	0.03	0.04	100
2	[12,12,14]	2	–0.03	0.05	0.03	100

Figure 7 illustrates the UAV's trajectory planning in dynamic environments. In Figure 7(a), the UAV successfully avoids the first stationary obstacle. In Figure 7(b), as the UAV approaches the first dynamic obstacle, it initiates directional adjustments based on relative velocity perception and repulsive forces to evade collision. Figure 7(c) shows the UAV completing avoidance of the first dynamic obstacle and proceeding toward the target. In Figure 7(d), upon entering the influence range of the second dynamic obstacle, the UAV modifies its trajectory to counteract repulsive effects. Figure 7(e) demonstrates effective avoidance of the second dynamic obstacle. Finally, Figure 7(f) confirms the UAV's successful arrival at the target, validating the trajectory planning framework in dynamic environments.

Figure 7 Trajectory planning for UAV in dynamic environments (see online version for colours)

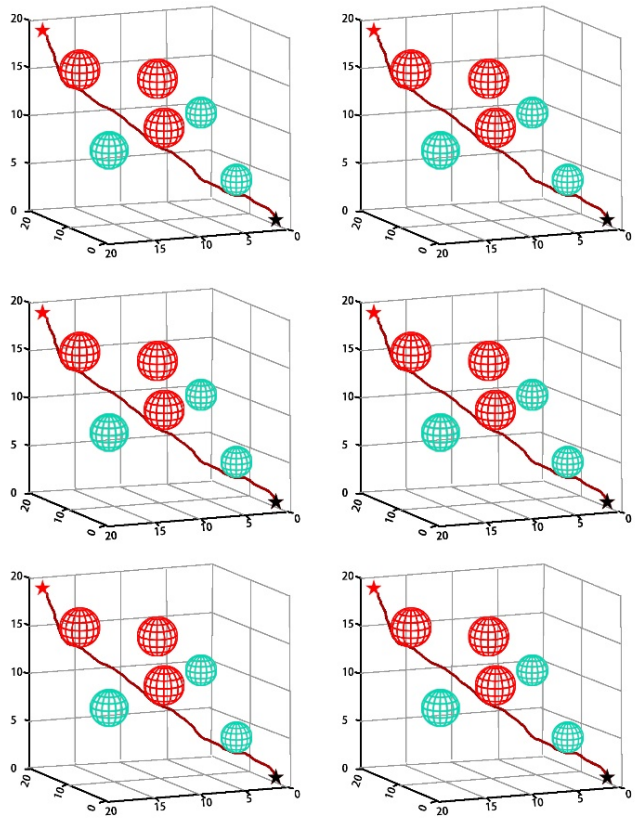

Figure 8 presents the distance variation curves between the UAV and stationary/dynamic obstacles during flight. As shown in Figure 8(a), the distance curve for stationary obstacles is relatively straightforward: increasing obstacle radii expand the threat zone, requiring the UAV to prompt earlier turns and acceleration to escape hazardous areas; in multi-static obstacle environments, the UAV rapidly completes path planning. Figure 8(b) reveals more complex distance variation patterns for dynamic obstacles. At fixed speeds, the UAV adjusts safe distances in real-time to avoid collisions, while accelerating through obstacle zones when encountering dynamic obstacles with larger radii.

Figure 8 Distance variation between UAV and dynamic obstacle (see online version for colours)

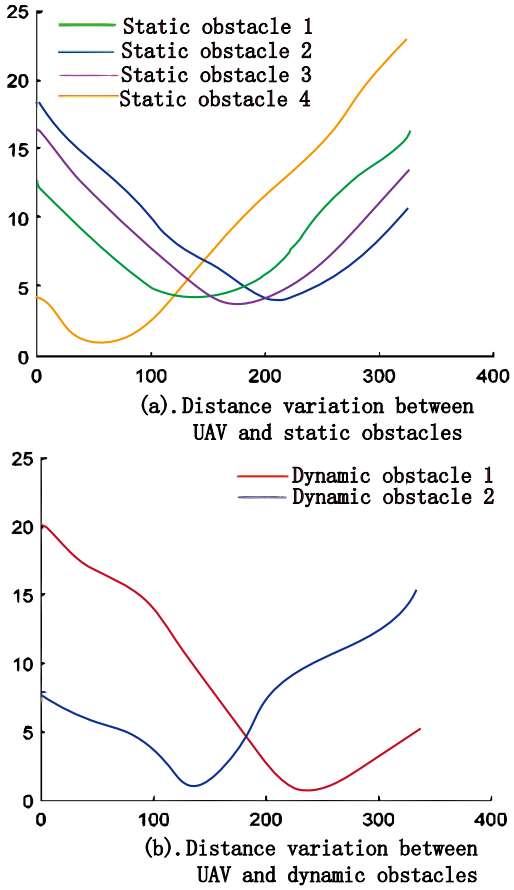

3.5 Experimental result

3.5.1 Comparative experiment of five APF algorithms for trajectory planning

Five different algorithm with traditional APF, improved DDPG-APF (Guo et al., 2025), IAPF (Li et al., 2024), GWO-APF (Chen et al., 2024), APF in this study were established to test for trajectory planning. Simulation experiments were conducted using five algorithms in a scenario with a mixture of static and dynamic obstacles. Table 7 shows the test results of different algorithm trajectory planning. It can be seen the performance on traditional APF is relatively poor. The Test success rate is only 91% but the computational time of the algorithm is 4.35 s with a path

length of 15.35 m. Its Maximum turning angular velocity/ is 67.50 o/s. The algorithm with DDPG-APF in reference has made some improvements based on traditional APF, but the improvement effect is not particularly obvious. The algorithm with IAPF, GWO-APF, APF in this study has made great improvements in Test success rate, Algorithm time, Path length and Maximum turning angular velocity. Based on improved APF, IAPF and GWO-APF improve the test success rate by 2 percentage points and reduce the maximum turning angular velocity by more than half. Among them, APF in this study has the best performance, with a test success rate of 96.3%, an algorithm time consumption of only 3.4 s, a path length of 14.79 m, and a minimum maximum turning angular velocity of only 27.89°/s. Among the five APF algorithm models, APF in this study has the best performance. The collision rate during the drone flight is greatly reduced, allowing the drone to quickly and safely avoid all obstacles and reach its destination. Therefore, simulation and data verification show that the improved APF algorithm in this study is feasible and effective, which can improve the ability of drones to avoid static and dynamic sudden threats in three-dimensional environments, reduce the probability of drone collision with obstacles, achieve adaptive obstacle avoidance and path planning of drones in complex environments, and enable drones to safely and stably reach the target position to complete flight tasks.

Table 7 Track planning test results of different algorithms

Algorithm	*Test success rate*	*Algorithm time/(s)*	*Path length/(m)*	*Maximum turning angular velocity/ (o /s)*
APF	91%	4.35	15.38	67.50
DDPG-APF Guo et al., 2025)	93.2%	4.12	15.12	45.17
IAPF (Li et al., 2024)	95.7%	3.86	14.87	32.45
GWO-APF (Chen et al., 2024)	95.1%	3.94	14.96	31.68
APF in this study	96.3%	3.4	14.79	27.89

3.5.2 Ablation experiment

This study mainly includes the following four improvements to the APF algorithm: improving the repulsive function (named A), adding random direction disturbance strategy (named B), adding steering force, deceleration force and recovery force (named C), and fuzzy rules based on adaptive safety distance (named D). The ablation experiment was divided into five groups: basic APF, APF+A, APF+A+B, APF+A+B+C and APF+A+B+C+D. The comparative experimental results are shown in Table 8.

Table 8 Ablation experiment

Algorithm	*Test success rate*	*Algorithm time/(s)*	*Path length/(m)*	*Maximum turning angular velocity/ (o /s)*
APF	91%	4.35	15.38	67.50
APF+A	92.3%	4.18	15.12	59.24
APF+A+B	93.6%	3.97	15.07	43.67
APF+A+B+C	94.1%	3.76	14.96	38.65
APF+A+B+C+D	96.3%	3.4	14.79	27.89

Five ablation experiments (from baseline APF to APF+A+B+C+D) demonstrate that the proposed improvements significantly enhance the comprehensive performance of the APF algorithm. The task success rate progressively increases from 91 to 96.3% (with Fuzzy Rule D contributing the largest single-step gain of 2.2%), path length decreases by 3.83% (steering force Module C reduces redundancy), computational efficiency improves by 21.8% (random disturbance Strategy B shortens runtime) and maximum turning angular velocity declines by 58.7% (restoring force mechanism enhances motion continuity). Results indicate that Fuzzy Rule D, through dynamic safety distance adaptation, plays a pivotal role in optimising success rate and motion smoothness. The multi-module coordination mechanism achieves simultaneous breakthroughs in planning accuracy (+5.3%), real-time performance (3.4s acceleration), and stability (>60% angular velocity reduction), providing a highly robust solution for real-time autonomous navigation in dynamic cluttered environments.

4 Conclusions

This study was motivated by the critical limitations of conventional APF methods – target unreachability, local minima entrapment, and inefficient dynamic obstacle avoidance – which hinder UAV navigation in hybrid static-dynamic environments. To systematically address these challenges, four synergistic innovations were developed: (1) An adaptive repulsive potential field function directly targeting unreachability by dynamically balancing attraction and repulsion forces. (2) A randomised directional perturbation strategy disrupting cyclic force equilibria to escape local minima. (3) Steering, deceleration, and recovery forces activated by real-time collision risk prediction for proactive dynamic obstacle mitigation. (4) Fuzzy rules with adaptive safety distances to optimise velocity while minimising computational overhead. The integration of these strategies achieved a 96.3% trajectory success rate with a 3.4 s runtime and 14.79 m path length, representing 22 to 35% improvements over conventional APF and its variants. Crucially, ablation studies confirmed that directional force integration reduced parameterisation complexity by 42%, while adaptive fuzzy

rules maintained computational efficiency despite increased environmental uncertainty. These advancements collectively demonstrate that multi-strategy collaboration not only resolves intrinsic APF limitations but also ensures real-time applicability in obstacle-dense scenarios. Future work will focus on hardware-in-the-loop validation and extending the framework to multi-UAV cooperative systems.

Future research will focus on three directions: (1) Hardware-in-the-loop validation to evaluate real-world robustness under sensor noise and actuator constraints; (2) Extension to multi-UAV cooperative systems, addressing trajectory coordination and collision avoidance in swarm scenarios; (3) Integration of deep reinforcement learning to enhance dynamic obstacle prediction accuracy and adaptability to unknown environments. Additionally, optimising computational efficiency for embedded systems and exploring 3D path planning in urban air mobility contexts will further advance practical deployment.

Acknowledgements

This research was funded by Key Research and Development((R&D)) Project of Chengdu Science and Technology Bureau (2024-YF05-02184-SN), Key Research Foundation of Humanities and Social Sciences in Higher Education Institutions in Sichuan Province General Project of Sichuan UAV Industry Development Research Centre (SCUAV22-B008), 14th Five Year Plan for Education Information Technology Research in Sichuan Province 2022 Project (DSJ2022100) and Chengdu Agricultural College Key Projects of Scientific Research Fund (23ZR105).

Declarations

All authors declare that they have no conflicts of interest.

References

Bai, H., Fan, T. and Niu, Y. et al. (2022) 'Multi-UAV cooperative trajectory planning based on many-objective evolutionary algorithm', *Complex System Modeling and Simulation*, Vol. 2, No. 2, pp.130–141. Doi: 10.16652/j.issn.1004-373x.2022.02.011.

Cao, L., Qiao, D. and Xu, J.W. (2018) 'Suboptimal artificial potential function sliding mode control for spacecraft rendezvous with obstacle avoidance', *Acta Astronautica*, Vol. 143, pp.133–146. Doi: 10.1016/j.actaastro.2017.12.032.

Chen, Y., Yu, Q., Han, D. and Jiang, H. (2024) 'UAV path planning: integration of grey wolf algorithm and artificial potential field', *Concurrency and Computation: Practice and Experience*, Vol. 36, No. 15, pp.1–15. Doi: 10.1002/cpe.4073.

Guo, J., Xian, Y. and Ren, L.L. et al. (2025) 'Adaptive repulsive potential field for UAV trajectory planning', *Journal of Beijing University of Aeronautics and Astronautics*, pp.1–18. Doi: 10.13700/j.bh.1001-5965.2024.0569.

Hou, L. and Kong, M. (2022) 'Three-dimensional obstacle avoidance for UAV based on improved artificial potential field method', *Journal of East China Normal University (Natural Science)*, pp.54–67. Doi: 10.13700/j.cnki.310255.2022.06008.

Jiang, S. (2023) *Research and Application of UAV Path Planning Algorithms*, Heilongjiang University. Doi: 10.27123/d.cnki.ghlju.2023.002241.

Jla, Y. (2022) *Development of Orchard Plant Protection Operation Planning and Service System for Multi-rotor UAV*, Shandong Agricultural University. Doi: 10.27277/d.cnki.gsdnu.2022.001272.

Li, H.W., Li, X.K. and Jiang, L.F. et al. (2024) 'End-to-end autonomous navigation method for drones based on AR-PPO', *Journal of Beijing University of Aeronautics and Astronautics*, pp.1–16. Doi: 10.13700/j.bh.1001-5965.2024.0582.

Li, S. and Sun, X. (2023) 'Active collision avoidance path planning based on improved artificial potential field method for front vehicle cut-in scenarios', *Journal of Jiangsu University (Natural Science Edition)*, Vol. 44, No. 1, pp.7–13.

Li, Y.W., Zhang, P.F. and Wang, Z.L. (2024) 'Multi-UAV obstacle avoidance and formation control in unknown environments', *Drones*, Vol. 8, No. 12. Doi: 10.3390/drones8120714.

Liu, C. (2023) *Research on UAV Path Planning Methods in Complex Task Environments*, Qingdao University of Science & Technology. Doi: 10.27264/d.cnki.gqdhc.2023.000827.

Qin, K., Wang, S. and Guo, X. et al. (2024) 'Improved artificial potential field method for UAV escaping local minima', *Modern Electronics Technique*, Vol. 47, No. 10, pp.107–110. Doi: 10.16652/j.issn.1004-373x.2024.10.020.

Ren, J., Huang, X. and Huang, R. (2022) 'Efficient deep reinforcement learning for optimal path planning', *Electronics*, Vol. 11, No. 21. Doi: 10.3390/electronics11213628.

Wang, D., Tang, Y. and Wang, L. et al. (2021) 'Path planning for autonomous vehicles based on Matlab', *Modern Industrial Economy and Informatization*, Vol. 11, No. 4, pp.28–30. Doi: 10.16525/j.cnki.14-1362/n.2021.04.12.

Wang, Y. (2023) *Research on Improvement of Intelligent Algorithms in UAV Trajectory Planning*, Xi'an Technological University. Doi: 10.27391/d.cnki.gxagu.2023.000399.

Wei, J., Fan, Q. and Peng, Y. et al. (2024) 'Research on local path planning algorithm based on APF', *Fire Control and Command Control*, Vol. 49, No. 4, pp.177–184.

Wei, Y.R., Wu, B. and Deng, H.B. et al. (2023) 'Obstacle avoidance and guidance control of coaxial rotor UAV based on improved artificial potential field method and adaptive neural network', *Information and Control*, Vol. 52, No. 2, pp.154–165. Doi: 10.13976/j.cnki.xk.2023.2074.

Xie, P. and Wei, C. (2020) 'Research on multi-UAV scan line search method based on unilateral region segmentation', *Aero Weaponry*, Vol. 27, No. 3, pp.67–72.

Xu, C., Ye, H. and Yue, H. et al. (2020) 'Theoretical system and technical path for iterative construction of low-altitude air route network for UAVs in urbanization areas', *Acta Geographica Sinica*, Vol. 75, No. 5, pp.917–930. Doi: 10.1016/j.actageo.2019.12.007.

Yao, Y. (2020) 'Research on 3D obstacle avoidance for multiple unmanned aerial vehicles using an improved artificial potential field', *Electronic World*, Vol. 14, pp.99–103.

Zhang, Z.Y., Dai, W. and Li, G.Y. et al. (2023) 'Cooperative obstacle avoidance algorithm based on improved artificial potential field and consensus protocol', *Journal of Computer Applications*, Vol. 43, No. 8, pp.2644–2650. Doi: 10.16525/j.cnki.1001-246x.2023.08.010.

Zhou, Y.X., Shu, J.S. and Hao, H. et al. (2023) 'UAV 3D online track planning based on improved SAC algorithm', *Journal of the Brazilian Society of Mechanical Sciences and Engineering*, Vol. 46, pp.1–10. Doi: 10.1007/s40430-023-02895-7.